RESEARCH MEMORANDUM

EFFECTS OF TWO SPINNER SHAPES ON THE PRESSURE RECOVERY IN AN NACA 1-SERIES D-TYPE COWL BEHIND A THREE-BLADE PROPELLER AT MACH NUMBERS UP TO 0.80

By Ashley J. Molk and Robert M. Reynolds

Ames Aeronautical Laboratory
Moffett Field, Calif.

NATIONAL ADVISORY COMMITTEE
FOR AERONAUTICS

WASHINGTON

March 19, 1954

NACA RM A53L29a

NATIONAL ADVISORY COMMITTEE FOR AERONAUTICS

RESEARCH MEMORANDUM

EFFECTS OF TWO SPINNER SHAPES ON THE PRESSURE RECOVERY IN AN NACA 1-SERIES D-TYPE COWL BEHIND A THREE-BLADE PROPELLER AT MACH NUMBERS UP TO 0.80

By Ashley J. Molk and Robert M. Reynolds

SUMMARY

An investigation has been conducted to determine the effects of two spinner shapes on the pressure recovery in an NACA 1-series D-type cowl behind a three-blade propeller with fairly thick shanks. The spinner shapes considered were an NACA 1-series spinner and a spinner more nearly conical than the 1-series spinner. Platform-type junctures were used between the propeller and the spinner. Ram-recovery ratio was measured at the cowl inlet with the propeller removed and with the propeller operating. Data were obtained at Mach numbers from 0.20 to 0.80, at inlet velocity ratios from 0.29 to 1.37, and at a Reynolds number of 1.17 million based on the maximum diameter of the cowl. The propeller was operated at various advance ratios for blade angles from 33° to 58.5°.

For the test range of Mach numbers, the ram-recovery ratios of the cowling-spinner combinations with the propeller removed were above 0.96 with either spinner for inlet velocity ratios greater than 0.6, and were about 0.005 higher for the more nearly conical spinner than for the NACA 1-series spinner. The addition of the operating propeller generally resulted in lower ram-recovery ratios at the cowl inlet. With the propeller operating, the recoveries with the more nearly conical spinner were significantly higher than with the 1-series spinner for all test conditions. At near design conditions, the ram-recovery ratios with the more nearly conical spinner were 0.03 to 0.05 higher than with the NACA 1-series spinner. The inlet velocity ratio (0.6) below which there were excessive recovery losses was little affected by spinner shape.

INTRODUCTION

Turboprop-powered airplanes have the common design problem of providing efficient air induction for the turbine engine. The inlet efficiency of D-type cowlings, in addition to being influenced by variations in the geometry of the cowling, of the propeller-blade shanks, and of the propeller-spinner juncture, is affected by the shape of the spinner.

Numerous data have been reported concerning the pressure recoveries for cowlings with NACA 1-series spinners (refs. 1 to 4). Some data are also available (refs. 5 and 6) concerning the pressure recoveries for cowlings with other spinner shapes, such as elliptic, parabolic, and conic. It was shown in reference 6 that the inlet pressure-recovery characteristics were better with conical spinners than with elliptic or parabolic spinners. This was the result of higher pressures acting on the cones, so that the boundary layer on the cones moved against a less adverse pressure gradient and, therefore, did not separate as readily. In designing a conical spinner for a turboprop installation, however, the necessity for clearance between the spinner and the propeller hub usually dictates a spinner of excessive base diameter for the minimum cowl size or else an undesirably long spinner of small cone angle for which there would probably be little improvement in recovery over an elliptic shape. It was thought, therefore, that as a compromise a modified conical shape might have some of the better flow characteristics of the conical shape, while retaining the compactness and the gradual transition to a cylindrical shape at the inlet characteristic of the elliptic profile.

An investigation was made to compare the effects of an NACA 1-series and a modified conical spinner on the ram-recovery characteristics of an NACA 1-series D-type cowl behind a fairly thick-shanked, three-blade propeller. The investigation was conducted in the Ames 12-foot pressure wind tunnel at Mach numbers up to 0.80 for various inlet velocity ratios, advance ratios, and blade angles. The angle of attack was 0°.

Some of the results of this investigation have been published previously in reference 7.

NOTATION

A cross-sectional area in a plane perpendicular to the model center line

[redacted]

a	speed of sound[1]
b	blade width
c_{l_d}	blade-section design lift coefficient
D	propeller diameter
H	total pressure[1]
$\frac{H_1 - p}{H - p}$	ram-recovery ratio
h	maximum thickness of blade section
J	advance ratio, $\frac{V_o}{nD}$
M	Mach number, $\frac{V}{a}$
m	mass flow, ρAV
$\frac{m_1}{m}$	mass-flow ratio, $\frac{\rho_1 A_1 V_1}{\rho A_1 V}$
n	propeller rotational speed
p	static pressure[1]
R	propeller tip radius
r	radius from center of rotation
T_a	thrust of the propeller-spinner combination in the presence of the cowling, corrected for the drag of the spinner
T_{c_a}	apparent propeller thrust coefficient, $\frac{T_a}{\rho V^2 D^2}$
V	velocity[1]
V_o	equivalent free-air velocity (datum velocity corrected for wind-tunnel-wall constraint on the propeller slipstream)

[1]As used herein, values of a, H, p, V, and ρ appearing without subscripts refer to conditions in the wind-tunnel air stream at a datum velocity, where the datum velocity has been corrected for blockage of the cowling but is uncorrected for wind-tunnel-wall constraint on the propeller slipstream. (See ref. 8.)

[redacted]

$\frac{V_1}{V}$ inlet velocity ratio

β propeller-blade angle at 0.75 R

β_d design section blade angle

ρ mass density of air[1]

Subscripts

1 ram-recovery rake location

MODEL

The model used in the investigation was mounted in the Ames 12-foot pressure wind tunnel as shown in figure 1. The general model arrangement and the principal model dimensions are shown in figure 2. Coordinates for the cowling-spinner combinations are given in table I. The propeller was driven by the 1000-horsepower propeller dynamometer described in reference 9.

Design Conditions

The model used in the investigation simulated the propeller, spinner, and inlet geometry for a turboprop installation designed to operate at the following conditions:

Condition	Altitude, ft	Mach number	Blade angle, deg	Advance ratio	Engine air flow, lb/sec[a]	Inlet velocity ratio
Climb	0	0.26	33.5	1.22	54	1.00
Climb	25,000	.43	42.5	1.83	26	.70
Cruise	0	.42	45.5	2.43	54	.59
Cruise	25,000	.60	53.0	2.82	29	.49

[a]Pratt and Whitney T-34 turbine engine

Cowling-Spinner Combination

The NACA 1-62.8-070 cowling used in the investigation reported in reference 4 was used for this investigation. The maximum diameter of the

[1]See footnote 1 on page 3.

spinners was chosen to provide the inlet area required for the design inlet velocity ratios and air flow. The spinners were of nearly equal length, and were considered the smallest that would enclose a representative hub assembly. However, the 1-series spinner was nearly ellipsoidal in shape; whereas the modified conical spinner was based on a conical shape but differed from a cone by having a fairly small nose radius, a moderate longitudinal curvature through the main body, and by becoming tangent to a cylinder at the duct inlet.

Propeller and Propeller-Spinner Juncture

The propeller used for this investigation was a three-blade type designed by Hamilton Standard Division and it corresponded to the designation NACA 3.638-(675)(057)-0572. The design was for a full-scale propeller 15 feet in diameter, having NACA 64A-series sections over the inner portion of the blades, and NACA 16-series sections over the outer portion, with a transition between approximately 40 and 50 percent of the blade radius. A cuff was simulated over the inner portion of the blades, ending in a discontinuity at the 42-percent blade radius. Plan-form and blade-form curves for the propeller are given in figure 3.

The propeller-spinner juncture was of the platform type (fig. 2), having no twist, no taper, a thickness-chord ratio (h/b) of approximately 0.41, and a modified NACA 64-series airfoil section. The platforms were fixed to the spinners at a pitch angle of 83° from the plane of rotation, so as to be alined with the propeller-shank section when the blade angle was set at 48°. All surfaces defining the gap between the platforms and propeller-blade-shank sections were plane (fig. 2, detail "A").

Instrumentation

The instrumentation of the model was identical with that of the model described in reference 4, except that the total- and static-pressure rakes contained six tubes each instead of eight. The tubes of the total-pressure rakes were disposed radially across the duct and spaced in such a manner that each tube was in the center of an area equal to one twenty-fourth of the total duct area.

TESTS AND REDUCTION OF DATA

Pressure recoveries in the duct were measured for each spinner with the propeller removed and with the propeller in place and operating. With the propeller removed, data were obtained for inlet velocity ratios

[redacted]

from 0.29 to 1.35, and for Mach numbers from 0.20 to 0.80. With the propeller operating, tests were conducted with various blade angles, Mach numbers, inlet velocity ratios, and advance ratios as follows:

Propeller blade angle, deg	Mach number	Average inlet velocity ratio	Advance ratio	Thrust Coefficient
1-series spinner				
58.5	0.80	0.32 to 0.87	3.21 to 4.28	-0.006 to 0.013
58.5	.70	.34 to 1.02	2.80 to 4.45	-.006 to .031
53	.60	.33 to 1.12	2.40 to 3.65	-.008 to .047
53	.50	.50	2.09 to 3.73	-.008 to .077
53	.40	.52	1.81 to 3.77	-.007 to .104
48	.60	.54	2.43 to 2.93	-.007 to .019
48	.50	.29 to 1.18	2.06 to 3.08	-.007 to .058
[a]48	.50	.39 to 1.26	2.05 to 2.98	-.006 to .060
48	.40	.51	1.65 to 3.01	-.005 to .114
43	.50	.51	2.08 to 2.58	-.010 to .026
43	.40	.51 to 1.24	1.62 to 2.67	-.012 to .096
33	.20	.41 to 1.35	0.79 to 1.98	-.027 to .425
Modified conical spinner				
58.5	0.80	0.31 to 0.89	3.16 to 4.28	-0.005 to 0.015
58.5	.70	.33 to 1.07	2.84 to 4.60	-.006 to .033
53	.60	.31 to 1.15	2.44 to 3.68	-.007 to .048
48	.50	.30 to 1.22	2.00 to 3.10	-.008 to .067
43	.40	.41 to 1.25	1.63 to 2.58	-.008 to .095
33	.20	.40 to 1.37	0.82 to 1.89	-.017 to .394

[a]Platform gap sealed

All the tests were conducted with the model at an angle of attack of 0° and with a Reynolds number of 1.17 million based on the maximum diameter of the cowl.

The datum Mach number and velocity were corrected for blockage effects of the cowling as in reference 8. In no case did this correction exceed 1 percent. For the computation of advance ratio, the datum velocity was corrected for wind-tunnel-wall constraint of the propeller slipstream by the method of reference 10. The ratio between free-air velocity and datum velocity is shown in figure 4.

The methods used in determining the thrust of the propeller-spinner combination in the presence of the cowling were the same as described in reference 8. The drag of the spinner in the presence of the cowling,

[redacted]

expressed in thrust-coefficient form, varied between $T_{c_a} = -0.0020$ and -0.0048, depending on Mach number and inlet velocity ratio.

The inlet velocity ratios were calculated by the method of reference 11. Mass-flow ratio m_1/m can readily be derived from inlet velocity ratio by the use of figure 4 of reference 11.

The variation of ram-recovery ratio radially across the duct was computed by averaging the total-pressure readings from the four tubes at each of the six radial locations. All other values of ram-recovery ratio were computed from an average of the readings from all 24 total-pressure tubes, resulting in an area-weighted average.

RESULTS

The variation of ram-recovery ratio radially across the duct with the propeller removed is presented for the NACA 1-series spinner in figure 5 and for the modified conical spinner in figure 6, for various inlet velocity ratios and Mach numbers. Figure 7 shows ram-recovery ratio as a function of inlet velocity ratio for the two spinners with the propeller removed.

The variation of ram-recovery ratio radially across the duct for both spinners with the propeller operating is presented in figure 8 for various inlet velocity ratios, Mach numbers, and blade angles for the advance ratios for maximum propeller efficiency. The effects of advance ratio on ram-recovery ratio are presented in figures 9 and 10 for the 1-series spinner. Figures 11 and 12 show, for the 1-series spinner, the effects on ram-recovery ratio of sealing the gap between the propeller and the platform at a Mach number of 0.50 for the pitch setting for which the propeller and the platform were alined ($\beta = 48^\circ$). The variation of ram-recovery ratio with advance ratio is shown in figure 13 for the modified conical spinner. Typical variations of ram-recovery ratio with propeller thrust coefficient with the two spinners are shown in figure 14. Figure 15 presents a comparison of ram-recovery ratios obtained with the two spinners as a function of inlet velocity ratio. Although the blade angles and Mach numbers given in figure 15 differ somewhat from the design values, the ram-recovery ratios presented in figures 15(a), (b), (c), and (e) are for the advance ratios for design climb and cruise. The ram-recovery ratios presented in figures 15(d), (f), and (g) are for the advance ratios for maximum propeller efficiency.

DISCUSSION

The ram-recovery ratios for the cowling-spinner combinations with the propeller removed (fig. 7) were above 0.96 for both spinners at inlet velocity ratios greater than 0.6, and were about 0.005 higher for the modified conical spinner than for the 1-series spinner. The recoveries decreased rapidly as the inlet velocity ratio was decreased below 0.6. For the test range of Mach numbers there was no perceptible effect of compressibility on the pressure recovery with the propeller removed.

A comparison of the data presented in figures 7 and 15 shows that addition of the operating propeller resulted in lower ram-recovery ratios, except at a Mach number of 0.20. This loss in recovery may be attributed to a thickening of the spinner boundary layer (see figs. 5, 6, and 8) and other air flow disturbances caused by the propeller. However, higher recoveries were obtained at low Mach numbers (figs. 9(a) and 13(a)) as a result of the addition of energy to the air flow by the propeller at high rotational speed and a favorable blade angle.

With the propeller operating, the ram-recovery ratios for the cowl with the modified conical spinner were significantly higher than for the cowl with the 1-series spinner throughout the test range of conditions. At near design conditions, the difference in recovery ratio for the two spinners amounted to 0.03 to 0.05 (fig. 15). Due to thickening of the spinner boundary layer, the ram-recovery ratio with both spinners decreased rapidly as the inlet velocity ratio was decreased below 0.6. At near design conditions, the ram-recovery ratios were above 0.88 with the modified conical spinner and above 0.84 with the 1-series spinner (fig. 15). As the inlet velocity ratio was increased above 0.6 with the propeller operating, the recoveries with both spinners decreased gradually. This decrease at high inlet velocity ratios is not in accord with previously reported data (ref. 4), and is believed to have been due primarily to the influence of the gap between the propeller blades and the platform junctures, as evidenced by the data shown in figure 12. It may be noted here that, whereas the gap between the propeller and platform was constant at 0.025 inches for the model reported in reference 4, the gap for the model reported herein varied from 0.060 to 0.164 (fig. 2). At Mach numbers of 0.70 and 0.80, operation of the relatively thick propeller-blade shanks at speeds greater than the critical speed of the sections and at local blade angles of 93.5° also contributed to the recovery losses. Operation of the propeller at lower blade angles at these Mach numbers (requiring lower advance ratios) was not permissible because of structural limitations of the model propeller.

CONCLUDING REMARKS

The following remarks may be made regarding the results of the subject investigation:

With the propeller removed, the ram-recovery ratios obtained at inlet velocity ratios above 0.6 for both cowling-spinner combinations were in excess of 0.96 and were approximately 0.005 higher for the modified conical spinner than for the NACA 1-series spinner.

The addition of the operating propeller to the spinner-cowling combinations generally resulted in lower recoveries. However, at low Mach numbers the addition of energy to the air flow by the propeller in some instances resulted in higher recoveries than were obtained with the propeller removed.

The ram-recovery ratios for the cowl with the modified conical spinner were significantly higher than those with the 1-series spinner throughout the test range of operating conditions. At near design operating conditions, the difference in recovery ratio between the two spinners was 0.03 to 0.05.

For both spinners, thickening of the spinner boundary layer at inlet velocity ratios below 0.6 caused large recovery losses both with and without the operating propeller.

With the propeller operating, the ram-recoveries behind either spinner decreased as the inlet velocity ratio was increased above 0.6. The ram-recovery ratios at near design conditions were above 0.88 for the modified conical spinner and above 0.84 for the 1-series spinner.

Ames Aeronautical Laboratory
National Advisory Committee for Aeronautics
Moffett Field, Calif., Dec. 29, 1953

REFERENCES

1. Nichols, Mark R., and Keith, Arvid L., Jr.: Investigation of a Systematic Group of NACA 1-Series Cowlings With and Without Spinners. NACA Rep. 950, 1949. (Formerly NACA RM L8A15)

[redacted]

2. Keith, Arvid L., Jr., Bingham, Gene J., and Rubin, Arnold J.: Effects of Propeller-Shank Geometry and Propeller-Spinner Juncture Configuration on Characteristics of an NACA 1-Series Cowling-Spinner Combination With an Eight-Blade Dual-Rotation Propeller. NACA RM L51F26, 1951.

3. Bingham, Gene J., and Keith, Arvid L., Jr.: Effects of Compressibility at Mach Numbers Up to 0.8 on Internal-Flow Characteristics of a Cowling-Spinner Combination Equipped With an Eight-Blade Dual-Rotation Propeller. NACA RM L53E12, 1953.

4. Sammonds, Robert I., and Molk, Ashley J.: Effects of Propeller-Spinner Juncture on the Pressure-Recovery Characteristics of an NACA 1-Series D-Type Cowl in Combination With a Four-Blade Single-Rotation Propeller at Mach Numbers Up to 0.83 and at an Angle of Attack of 0°. NACA RM A52D01a, 1952.

5. Pendley, Robert E., and Robinson, Harold L.: An Investigation of Several NACA 1-Series Nose Inlets With and Without Protruding Central Bodies at High-Subsonic Mach Numbers and at a Mach Number of 1.2. NACA RM L9L23a, 1950.

6. Pendley, Robert E., Milillo, Joseph R., Fleming, Frank F., and Bryan, Carroll R.: An Experimental Study of Five Annular Inlet Configurations at Subsonic and Transonic Speeds. NACA RM L53F18a, 1953.

7. Reynolds, Robert M.: Preliminary Results of an Investigation of the Effects of Spinner Shape on the Characteristics of an NACA D-Type Cowl Behind a Three-Blade Propeller, Including the Characteristics of the Propeller at Negative Thrust. NACA RM A53J02, 1953.

8. Reynolds, Robert M., Sammonds, Robert I., and Kenyon, George C.: An Investigation of a Four-Blade Single-Rotation Propeller in Combination With an NACA 1-Series D-Type Cowling at Mach Numbers up to 0.83. NACA RM A53B06, 1953.

9. Reynolds, Robert M., Buell, Donald A., and Walker, John H.: Investigation of an NACA 4-(5)(05)-041 Four-Blade Propeller With Several Spinners at Mach Numbers Up to 0.90. NACA RM A52I19a, 1952.

10. Young, A. D.: Note on the Application of the Linear Perturbation Theory to Determine the Effect of Compressibility on the Wind Tunnel Constraint on a Propeller. RAE TN Aero. 1539, British, 1944.

11. Smith, Norman F.: Numerical Evaluation of Mass-Flow Coefficient and Associated Parameters from Wake Survey Equations. NACA TN 1381, 1947.

[redacted]

TABLE I.- COWLING-SPINNER COORDINATES

[Coordinates in inches]

Distance from leading edge of cowl, x_c	NACA 1-62.8-070 cowl, radius, r_c	Distance from leading edge of cowl, x_i	NACA 1-series inner lip, radius, r_i	Distance from leading edge of 1-series spinner, x_s	NACA 1-50-74.6 spinner, radius, r_s	Distance from leading edge of modified conical spinner, x_s	Modified conical spinner, radius, r_s	Distance from leading edge of platform juncture, x_p	Platform juncture ordinate, y_p
0	4.460	0	4.460	0	0	0	0	0	0
.020	4.581	.008	4.439	.063	.284	.065	.227	.125	.343
.039	4.628	.017	4.429	.105	.363	.121	.329	.249	.470
.059	4.666	.034	4.415	.157	.445	.181	.401	.498	.650
.078	4.697	.050	4.403	.209	.516	.241	.471	.996	.873
.098	4.723	.067	4.394	.261	.580	.303	.530	1.494	.985
.196	4.834	.084	4.386	.314	.641	.362	.594	1.992	1.019
.490	5.078	.101	4.378	.419	.751	.483	.700	2.490	.946
.980	5.377	.118	4.372	.627	.945	.725	.889	2.989	.803
1.372	5.569	.134	4.366	.837	1.114	.966	1.047	3.487	.628
1.764	5.727	.168	4.355	1.255	1.403	1.450	1.325	3.985	.435
2.156	5.866	.202	4.346	1.777	1.693	1.933	1.549	4.483	.240
2.548	5.993	.244	4.337	2.195	1.891	2.416	1.743	4.981	0
2.940	6.108	.277	4.331	3.136	2.271	3.382	2.062	---	---
3.332	6.215	.311	4.326	3.972	2.553	4.349	2.340	---	---
3.724	6.313	.344	4.323	4.913	2.817	5.307	2.597	---	---
4.116	6.403	.378	4.320	5.854	3.035	6.277	2.819	---	---
4.508	6.485	.420	4.320	6.690	3.192	7.248	3.008	---	---
4.900	6.560	---	---	7.526	3.316	8.197	3.173	---	---
5.684	6.694	---	---	8.572	3.425	9.167	3.307	---	---
6.468	6.802	---	---	9.408	3.478	10.139	3.426	---	---
7.252	6.885	---	---	9.826	3.494	10.613	3.476	---	---
8.036	6.946	---	---	10.244	3.499	10.814	3.499	---	---
8.820	6.985	---	---	10.453	3.499	---	---	---	---
9.800	7.000	---	---	---	---	---	---	---	---

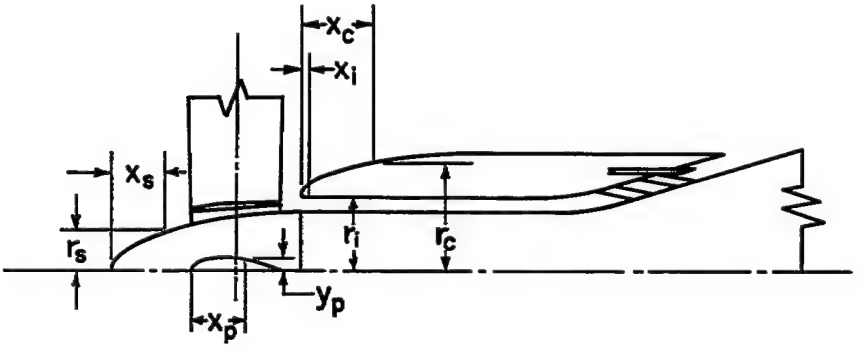

[redacted]

[redacted]

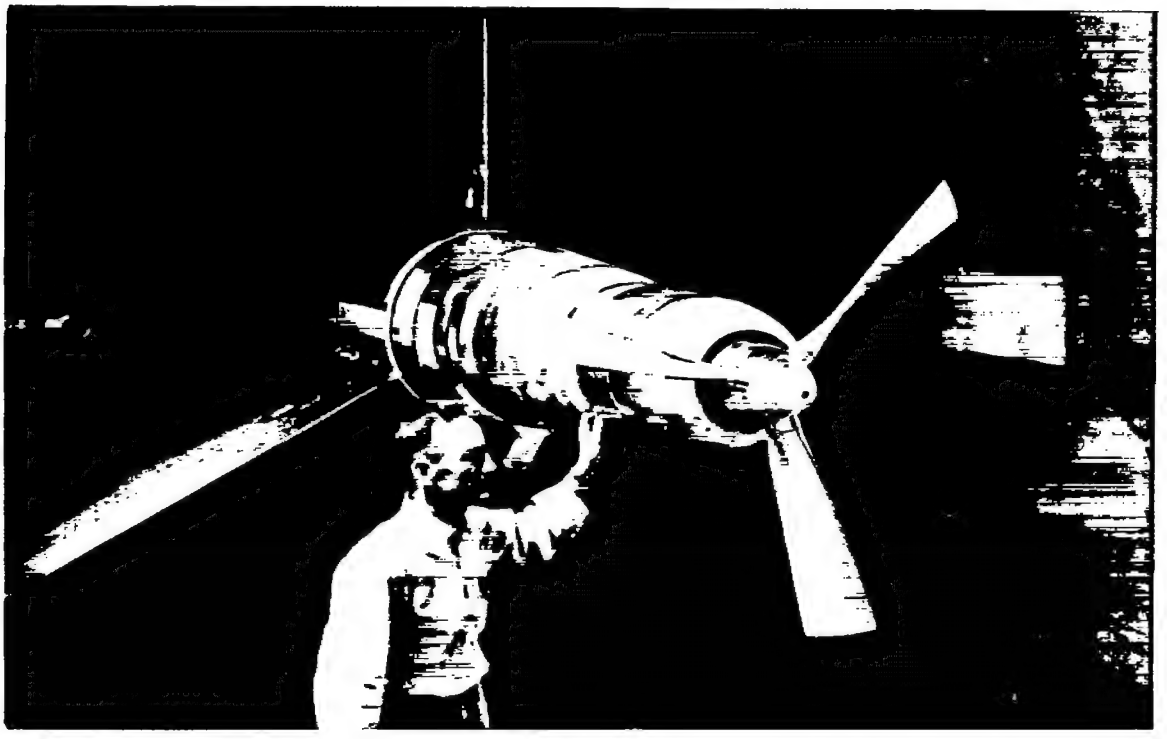

A-18329

Figure 1.- The model mounted on the 1000-horsepower propeller dynamometer in the 12-foot pressure wind tunnel.

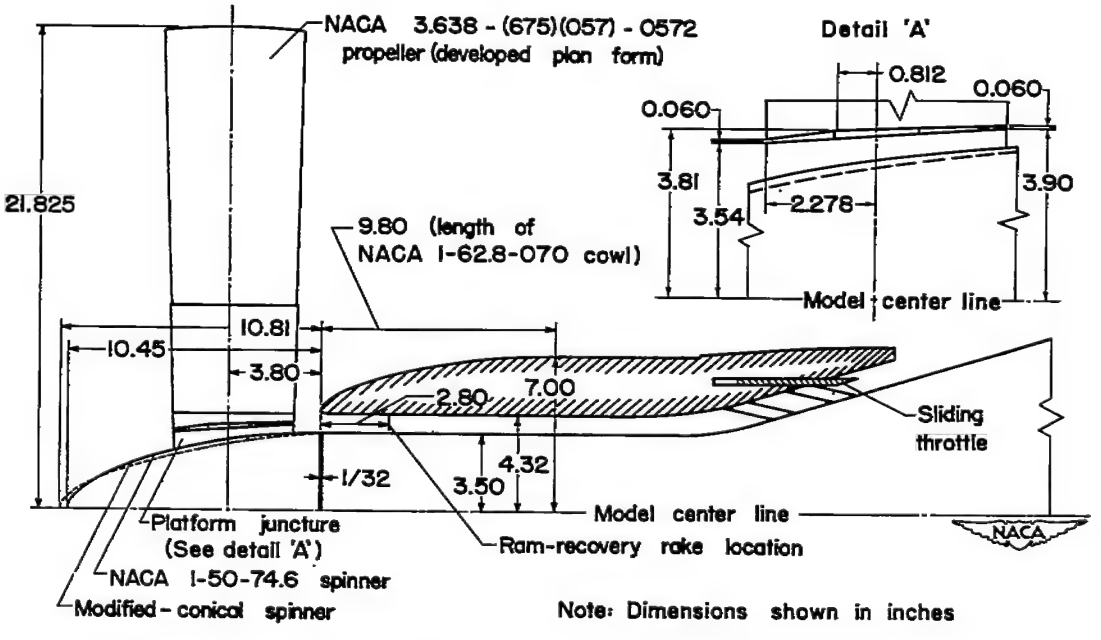

Figure 2.- Model arrangement.

[redacted]

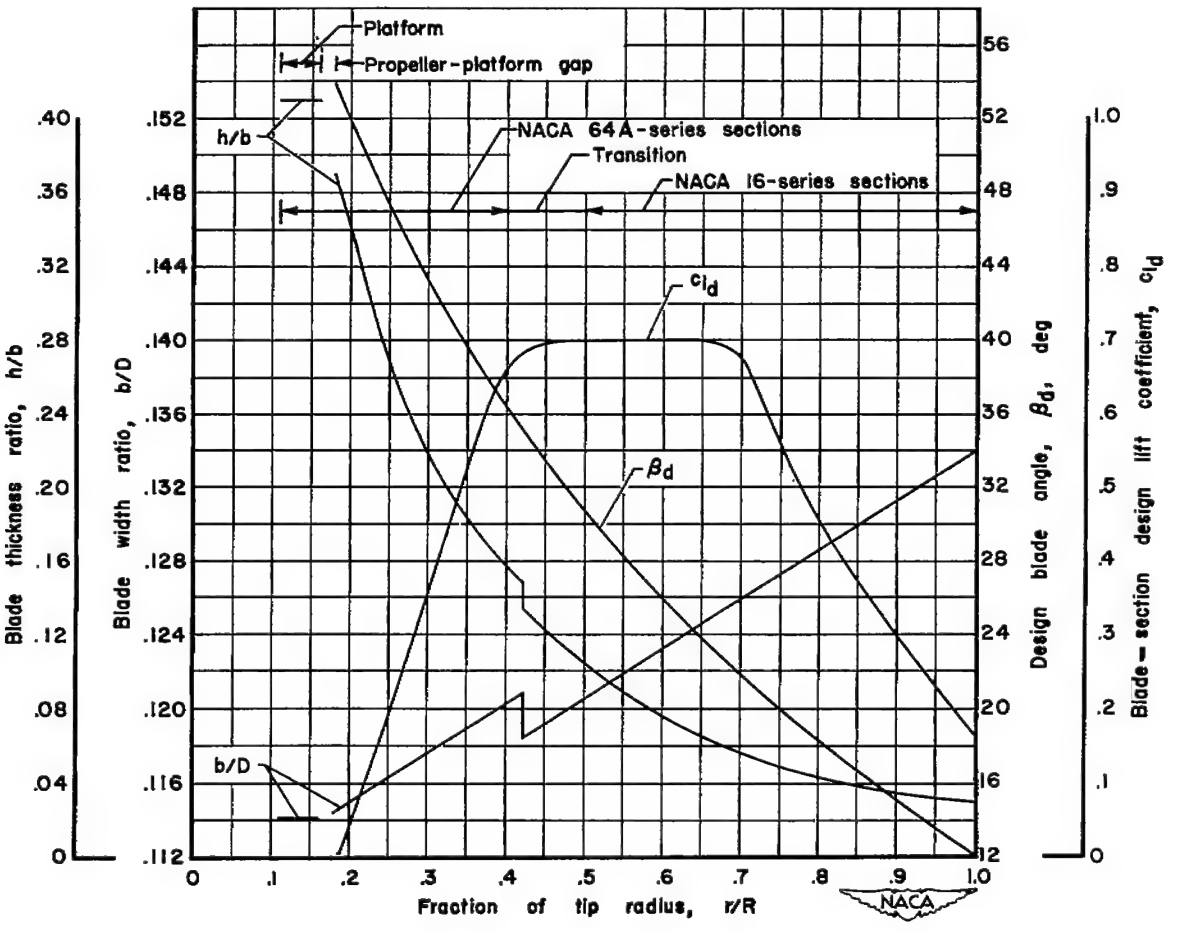

Figure 3.- Plan-form and blade-form curves for the model propeller having the designation NACA 3.638-(675)(057)-0572.

[redacted]

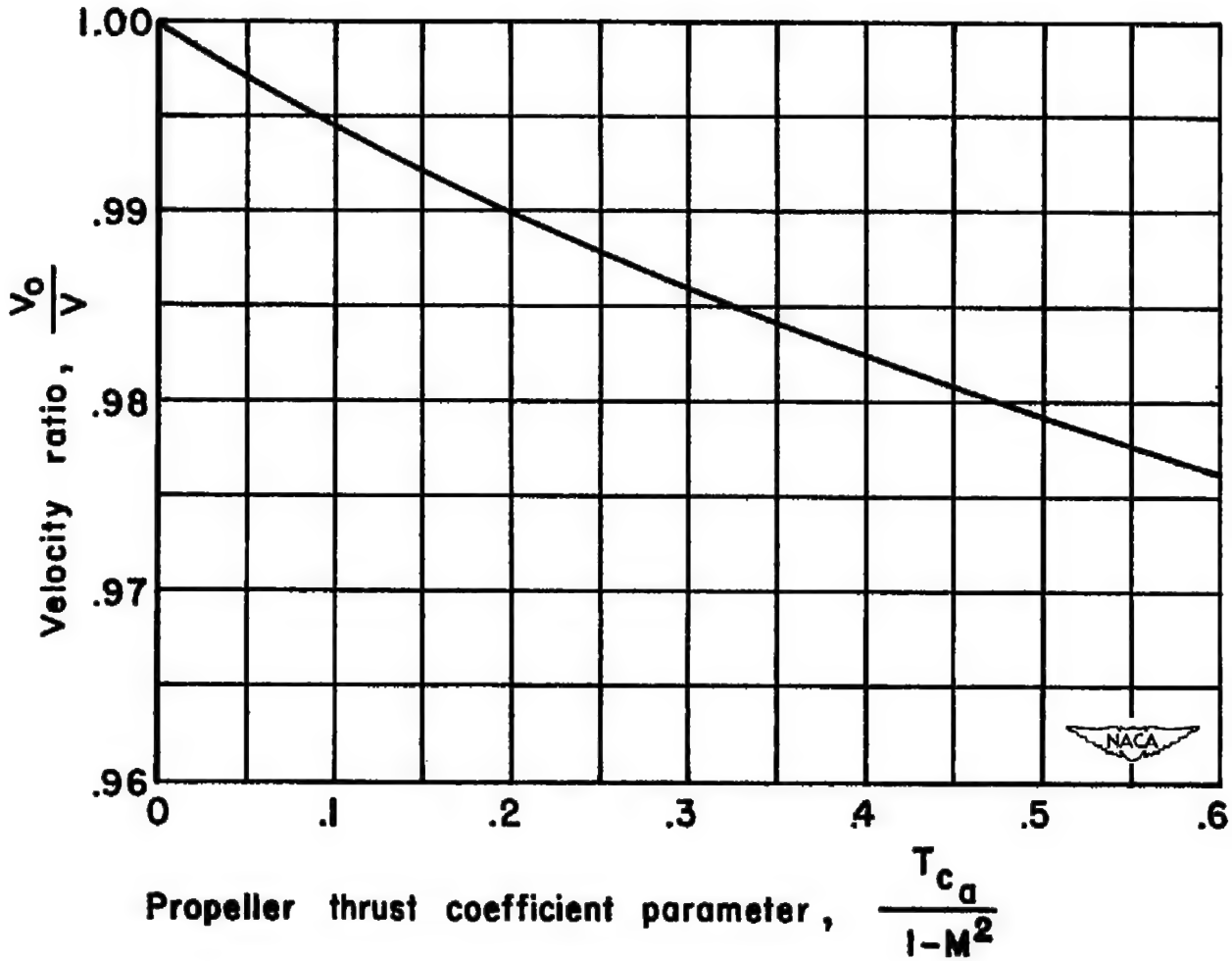

Figure 4.- Tunnel-wall-interference correction for a 3.638-foot-diameter propeller in the Ames 12-foot pressure wind tunnel.

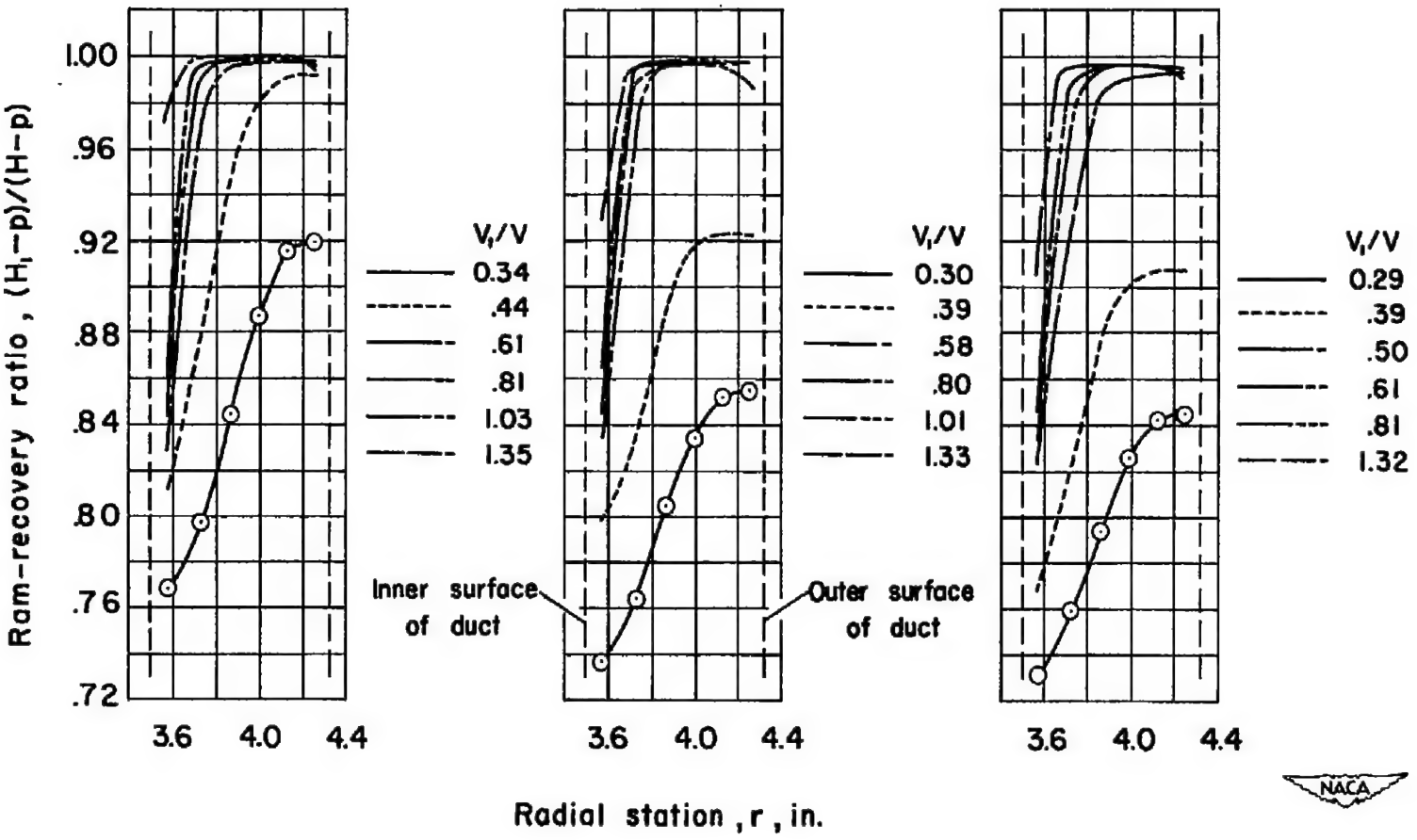

(a) M = 0.20 (b) M = 0.40 (c) M = 0.50

Figure 5.- The variation of the average ram-recovery ratio with radial station across the duct for various inlet velocity ratios; propeller removed, 1-series spinner.

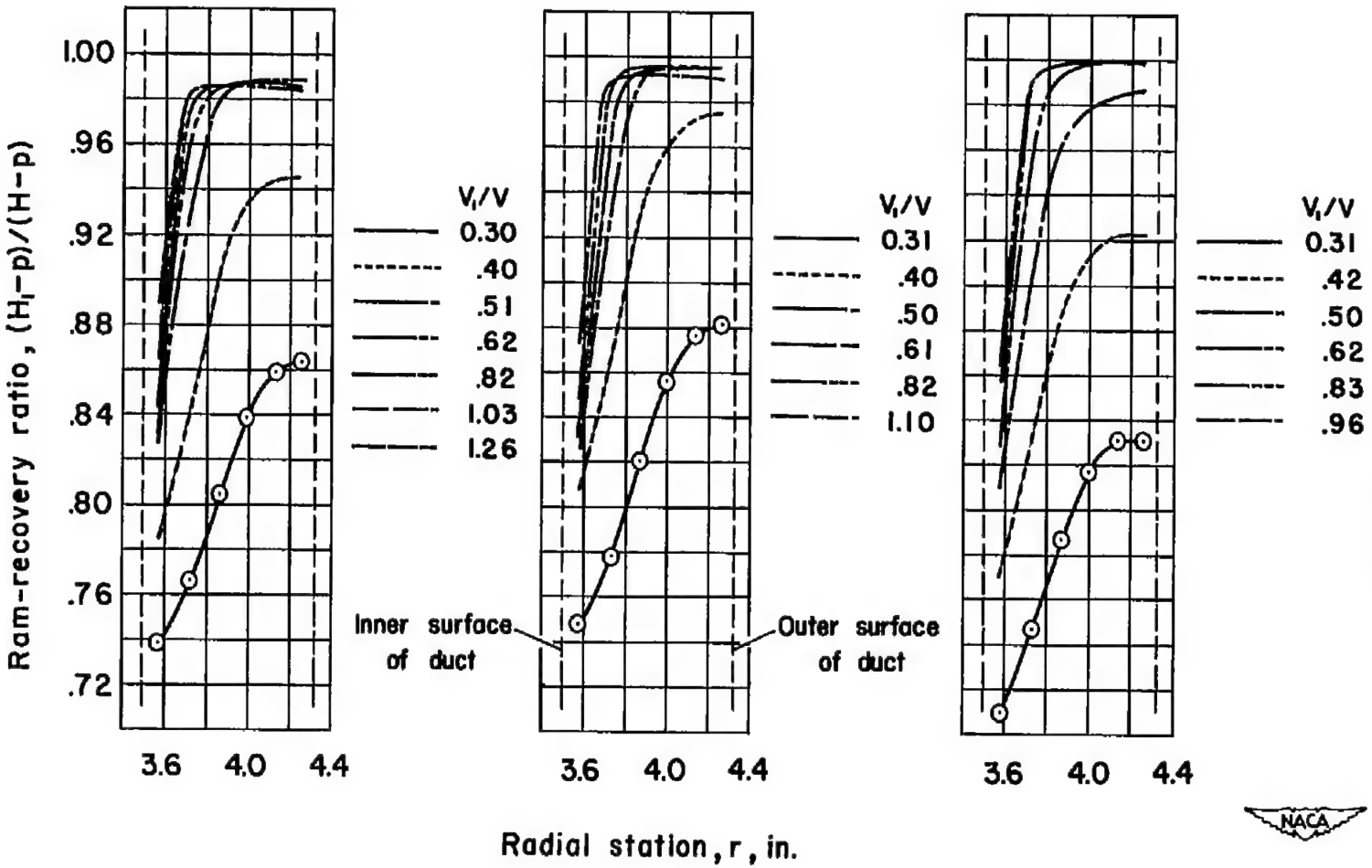

(d) M = 0.60

(e) M = 0.70

(f) M = 0.80

Figure 5.- Concluded.

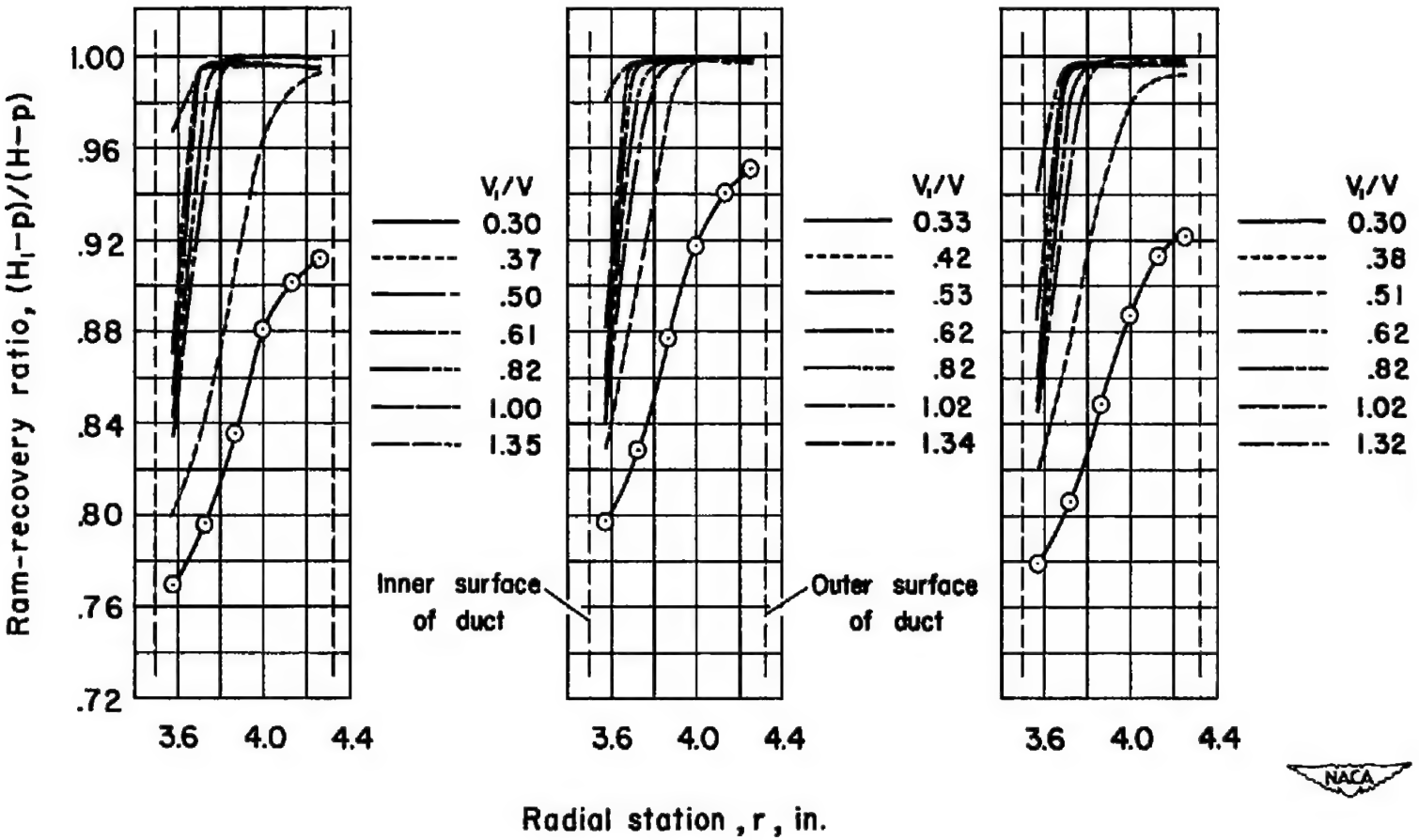

(a) M = 0.20 (b) M = 0.40 (c) M = 0.50

Figure 6.- The variation of the average ram-recovery ratio with radial station across the duct for various inlet velocity ratios; propeller removed, modified conical spinner.

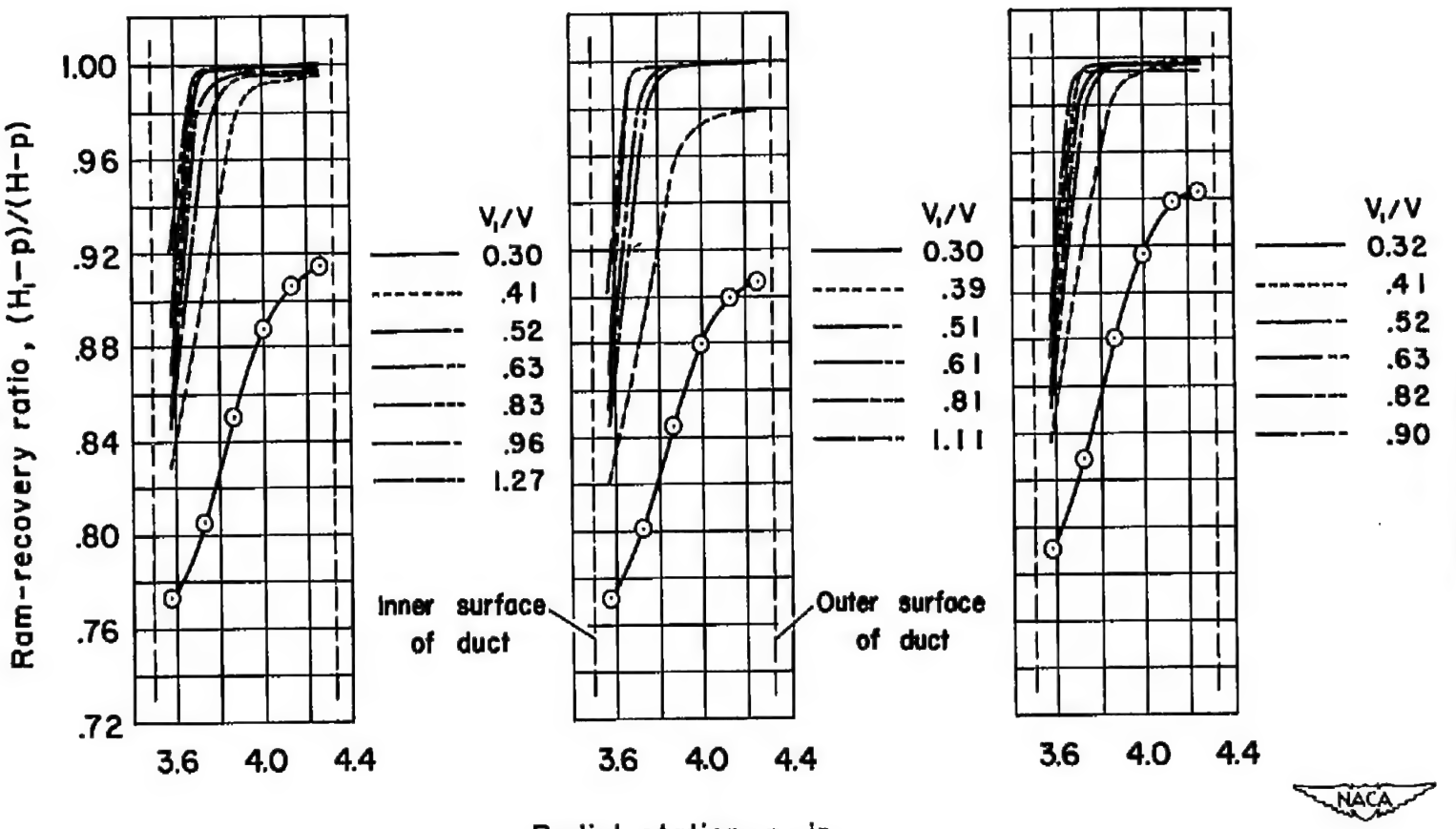

(d) M = 0.60

(e) M = 0.70

(f) M = 0.80

Figure 6.- Concluded.

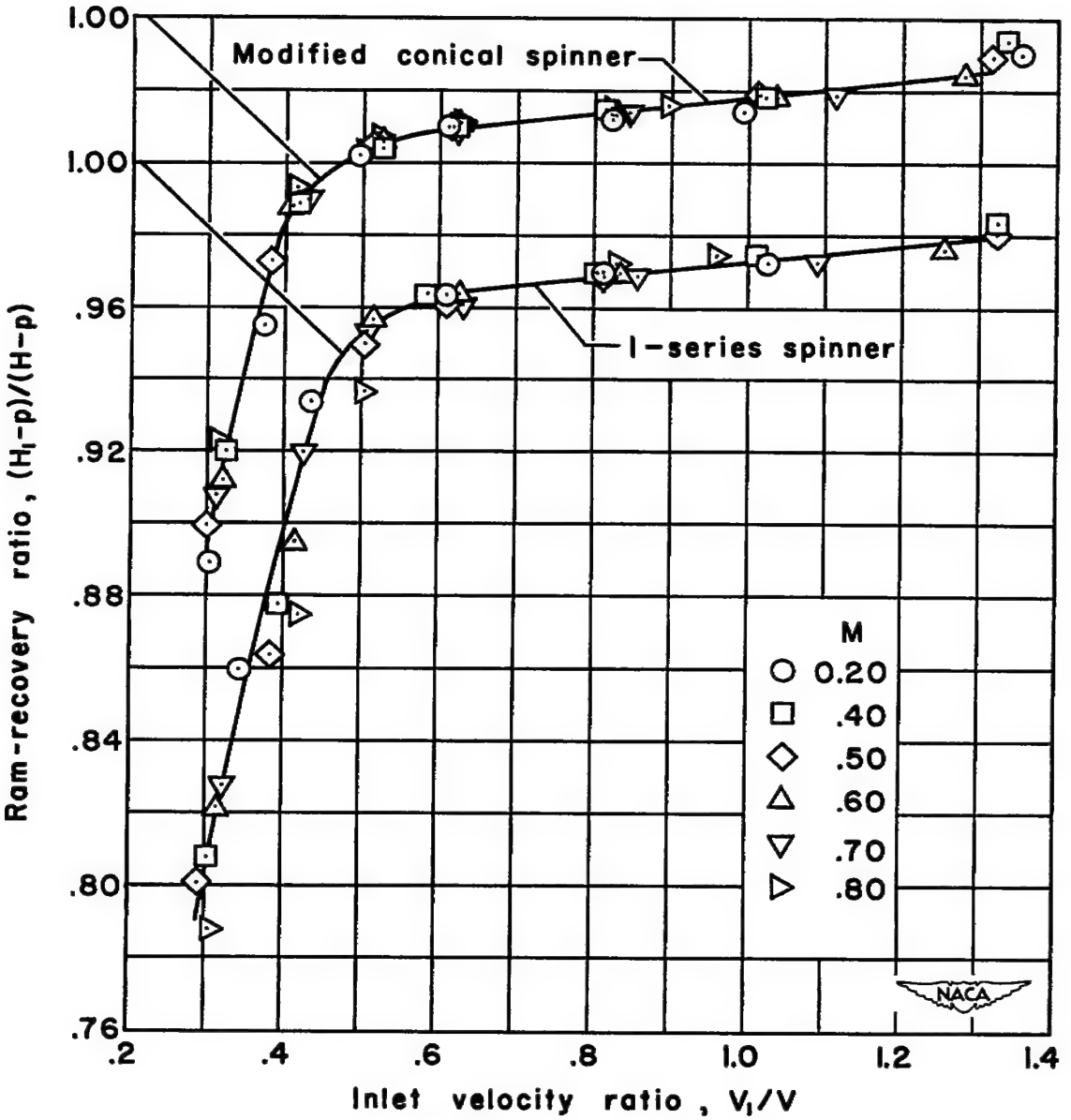

Figure 7.- The effect of inlet velocity ratio on the average ram-recovery ratio for the cowl with 1-series and modified conical spinners, propeller removed.

[redacted]

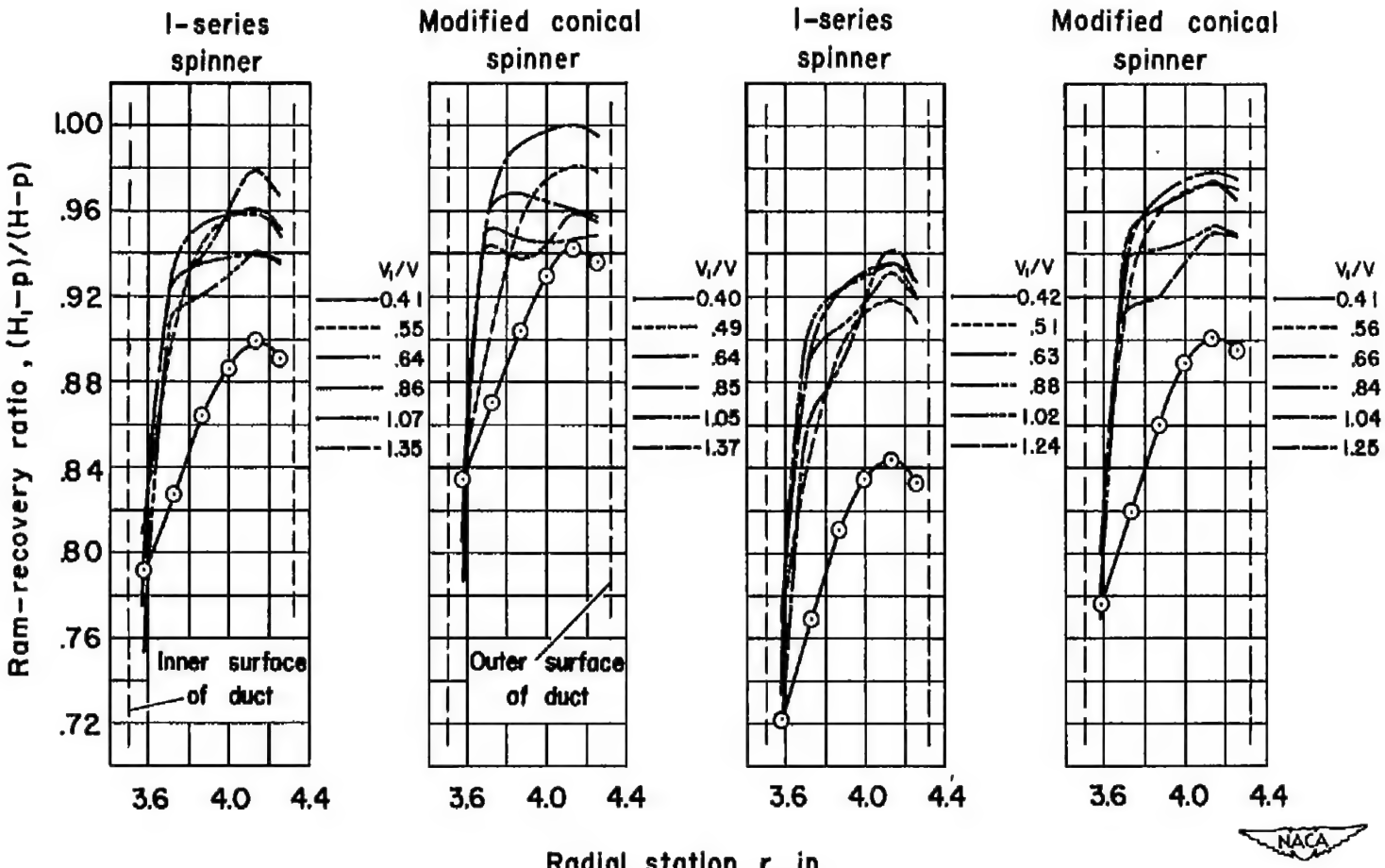

(a) M = 0.20, $\beta = 33^{\circ}$, J = 1.5.

(b) M = 0.40, $\beta = 43^{\circ}$, J = 2.0.

Figure 8.- The variation of the average ram-recovery ratio with radial station across the duct for various inlet velocity ratios; propeller operating, 1-series and modified conical spinners.

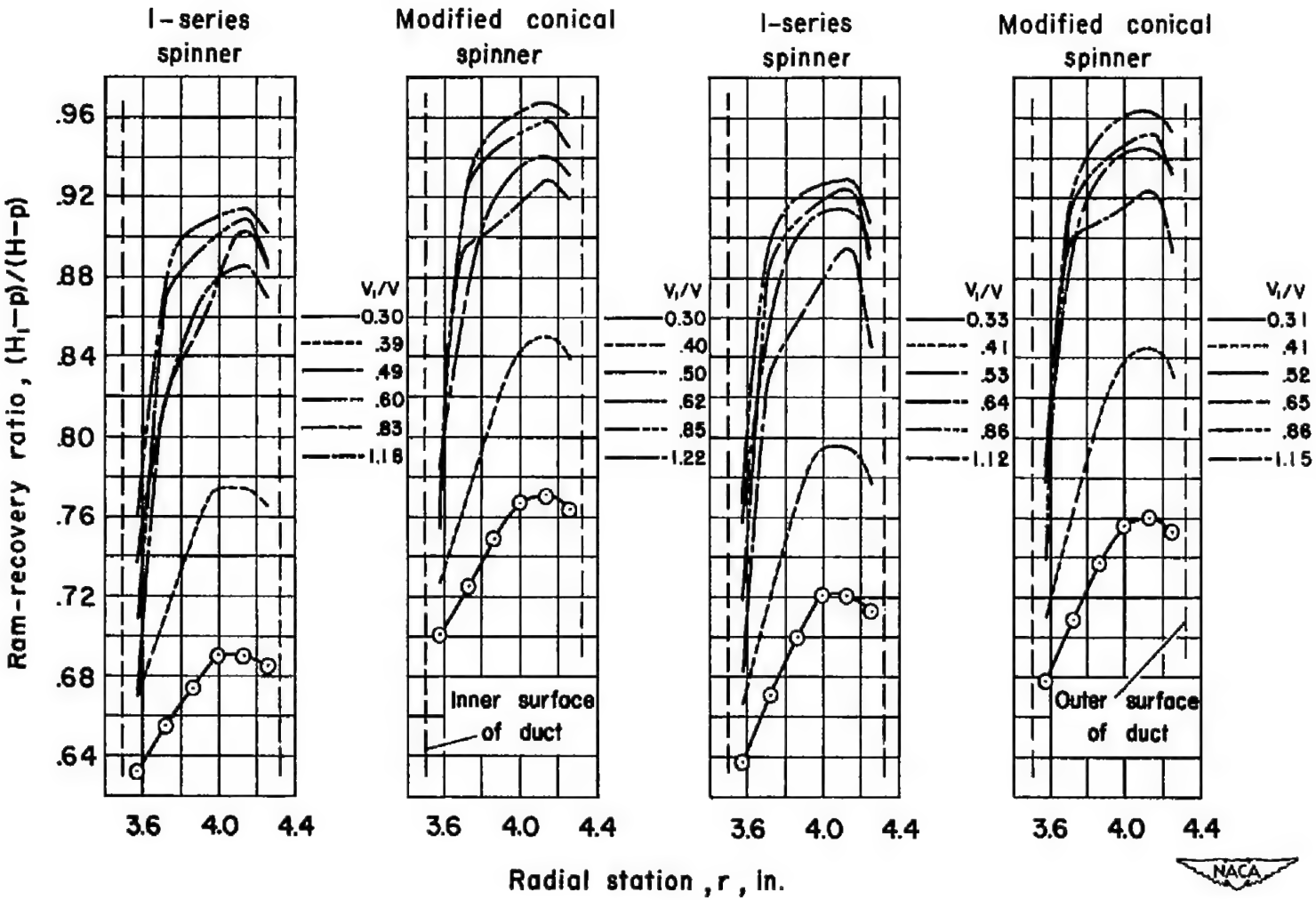

(c) M = 0.50, $\beta = 48^\circ$, J = 2.5.

(d) M = 0.60, $\beta = 53^\circ$, J = 2.8.

Figure 8.- Continued.

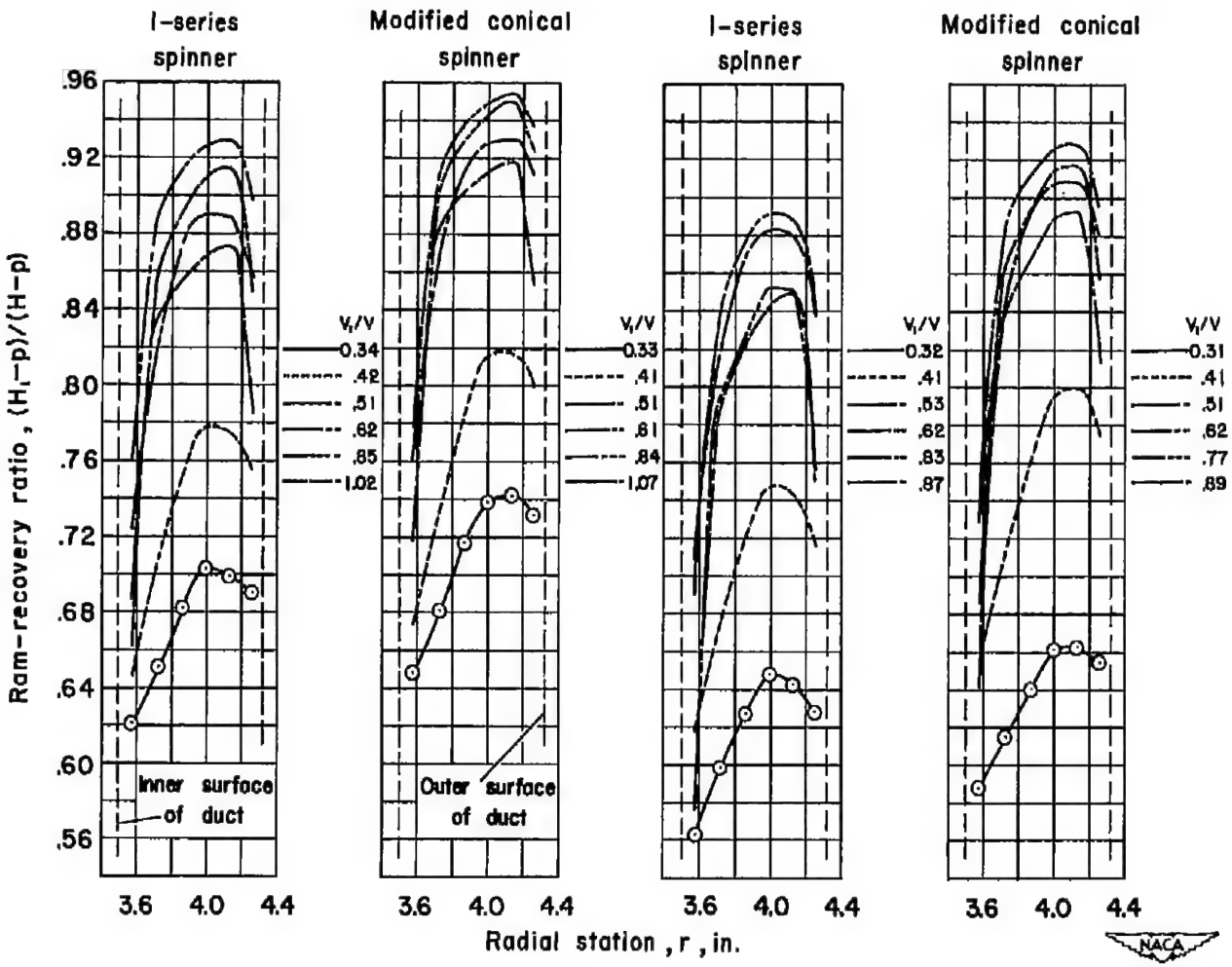

(e) M = 0.70, β = 58.5°, J = 3.4. (f) M = 0.80, β = 58.5°, J = 3.3.

Figure 8.- Concluded.

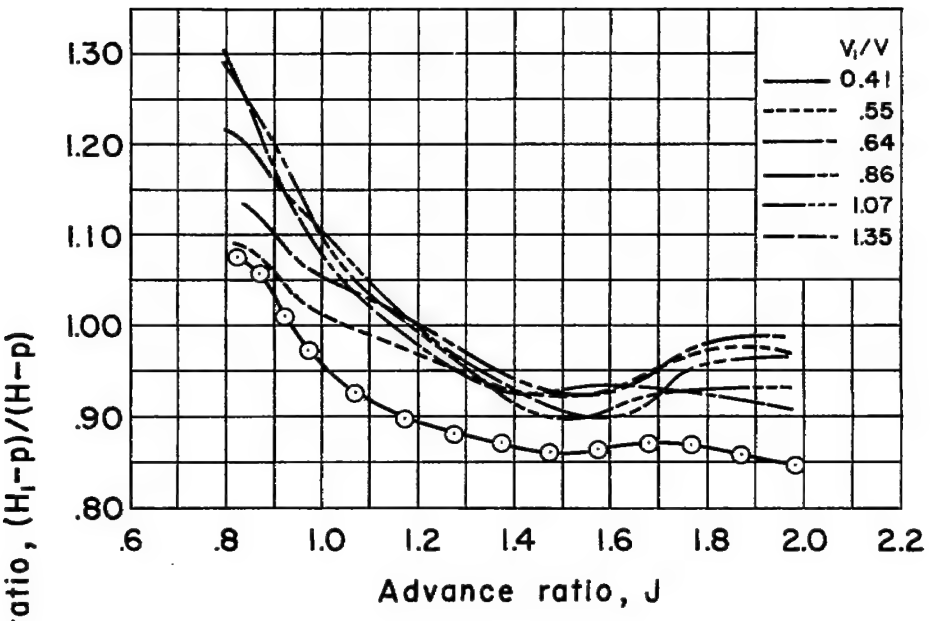

(a) M = 0.20, $\beta = 33^\circ$.

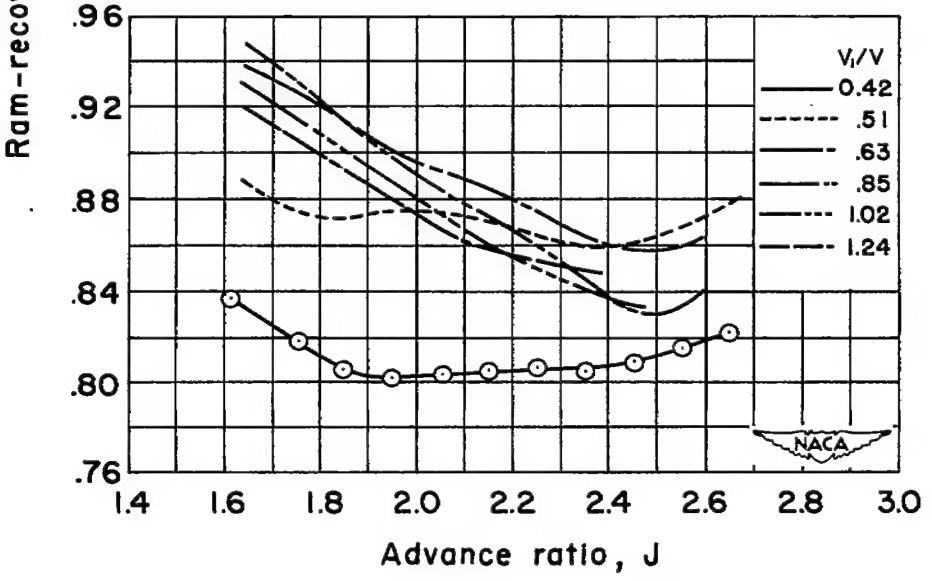

(b) M = 0.40, $\beta = 43^\circ$.

Figure 9.- The variation of the average ram-recovery ratio with advance ratio for various inlet velocity ratios, 1-series spinner.

[redacted]

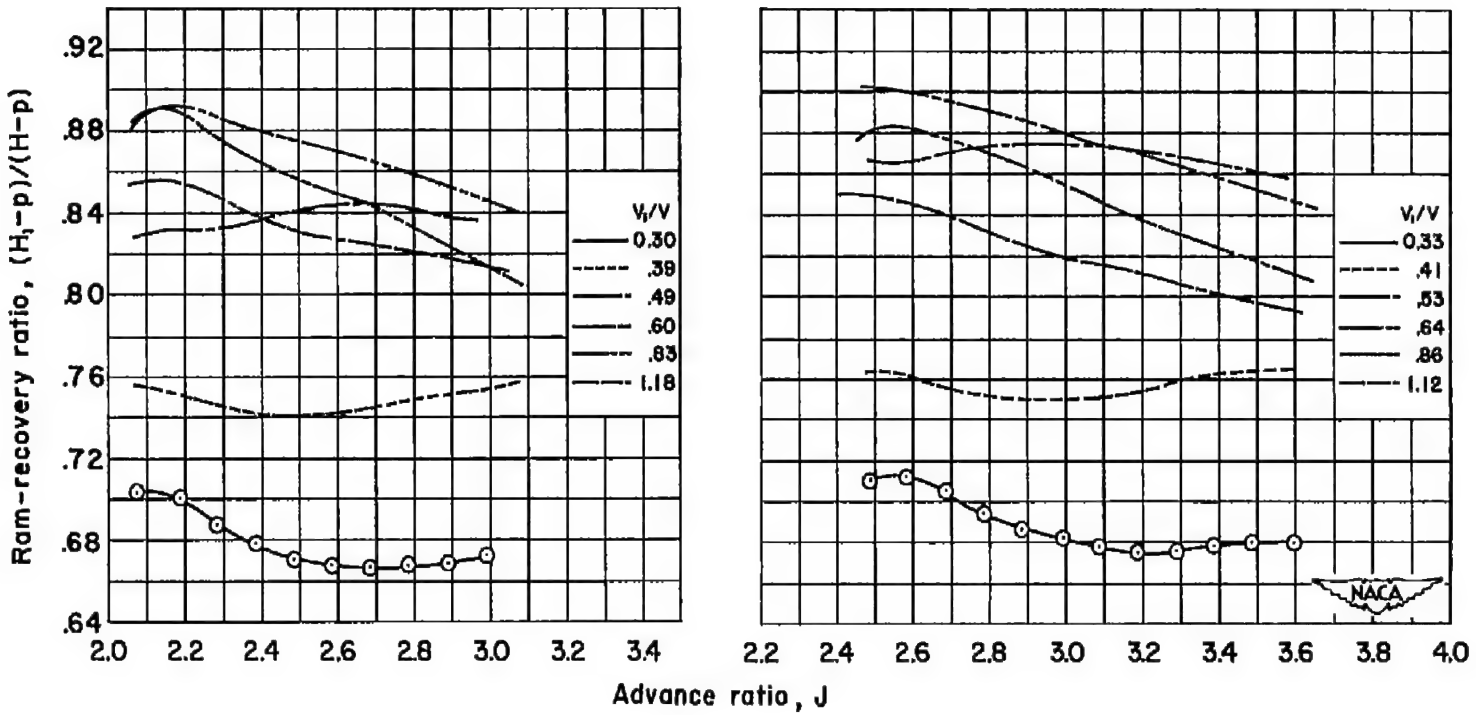

(c) M = 0.50, β = 48°.

(d) M = 0.60, β = 53°.

Figure 9.- Continued.

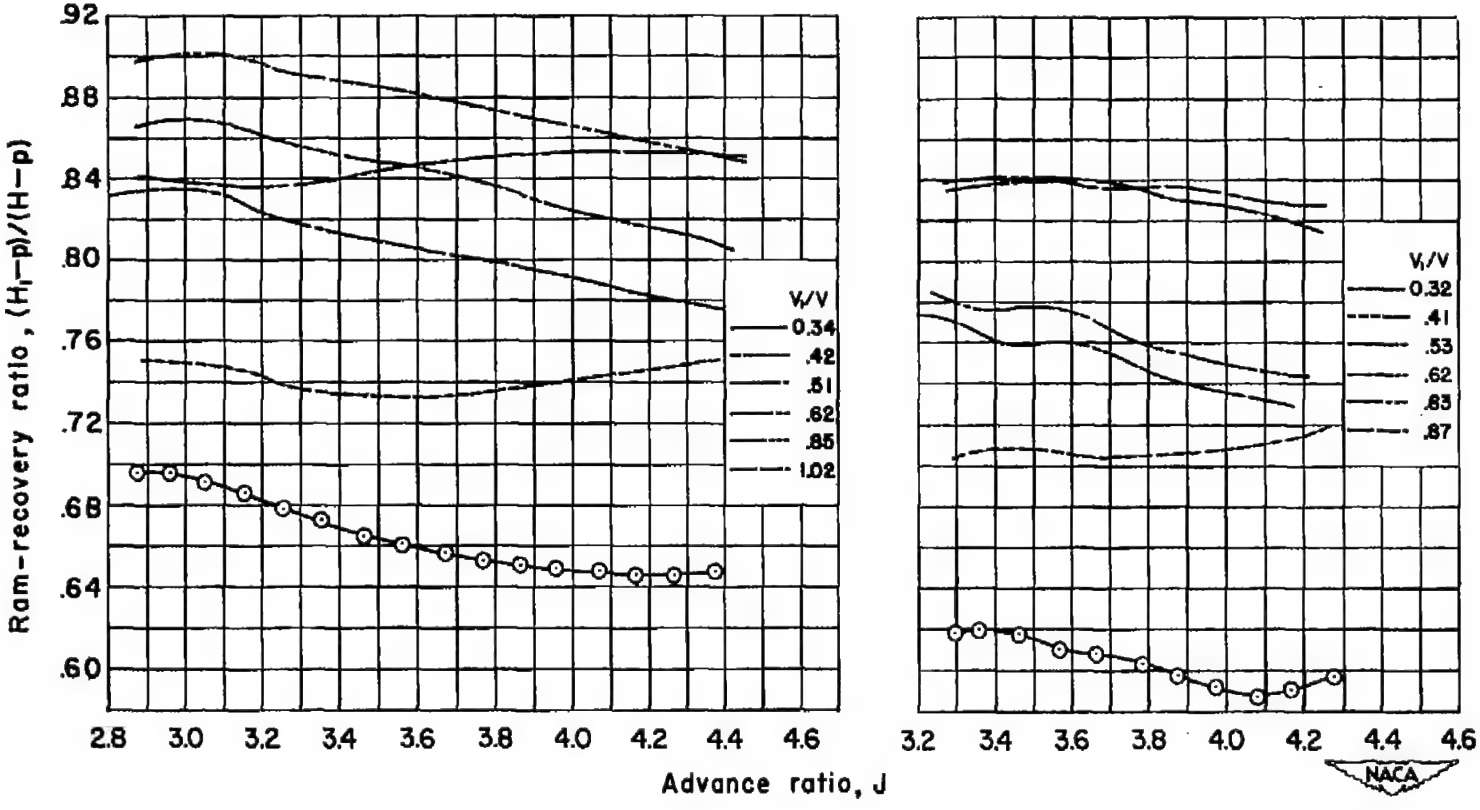

(e) M = 0.70, $\beta = 58.5^{\circ}$.

(f) M = 0.80, $\beta = 58.5^{\circ}$.

Figure 9.- Concluded.

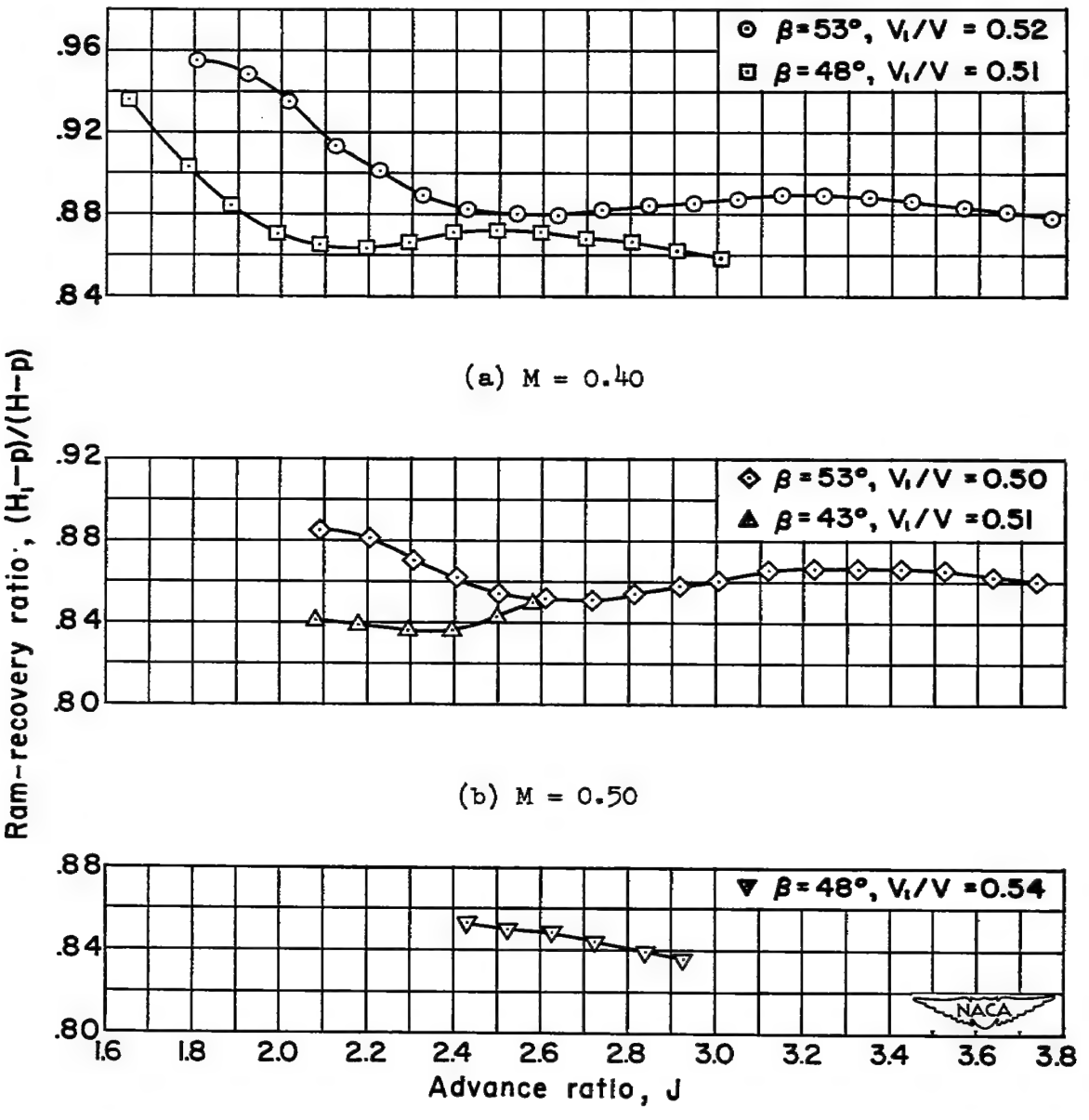

Figure 10.- The variation of the average ram-recovery ratio with advance ratio for various off-design combinations of blade angle and Mach number, 1-series spinner.

[redacted]

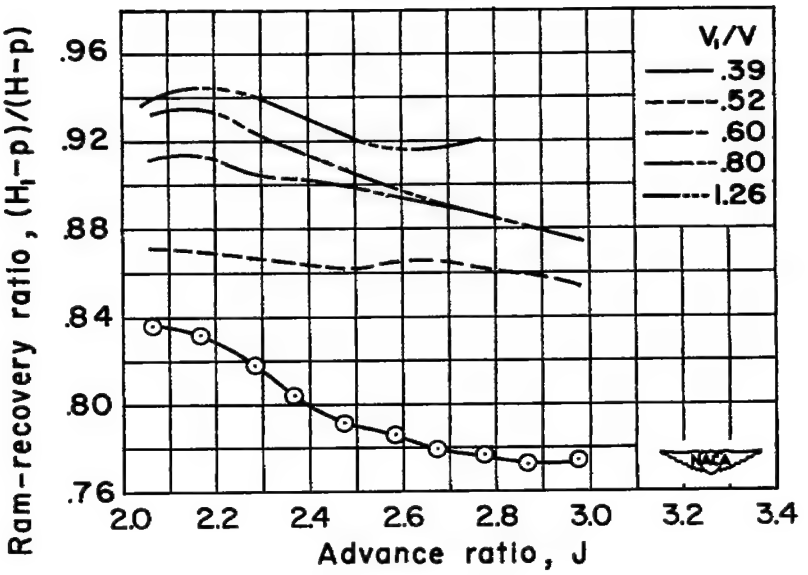

Figure 11.- The variation of the average ram-recovery ratio with advance ratio for the propeller alined with the platform and the propeller-platform gap sealed; M = 0.50, $\beta = 48^{\circ}$, 1-series spinner.

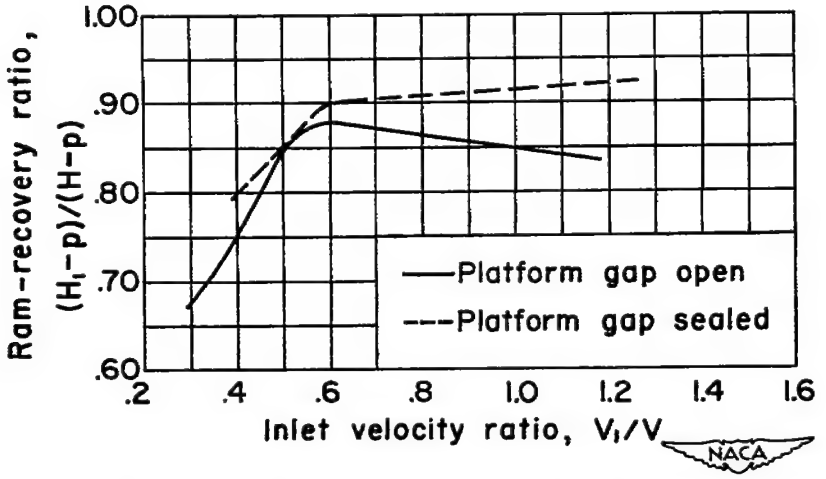

Figure 12.- The effect of sealing the propeller-platform gap on the variation of the average ram-recovery ratio with inlet velocity ratio; M = 0.50, $\beta = 48^{\circ}$, J = 2.45, 1-series spinner.

[redacted]

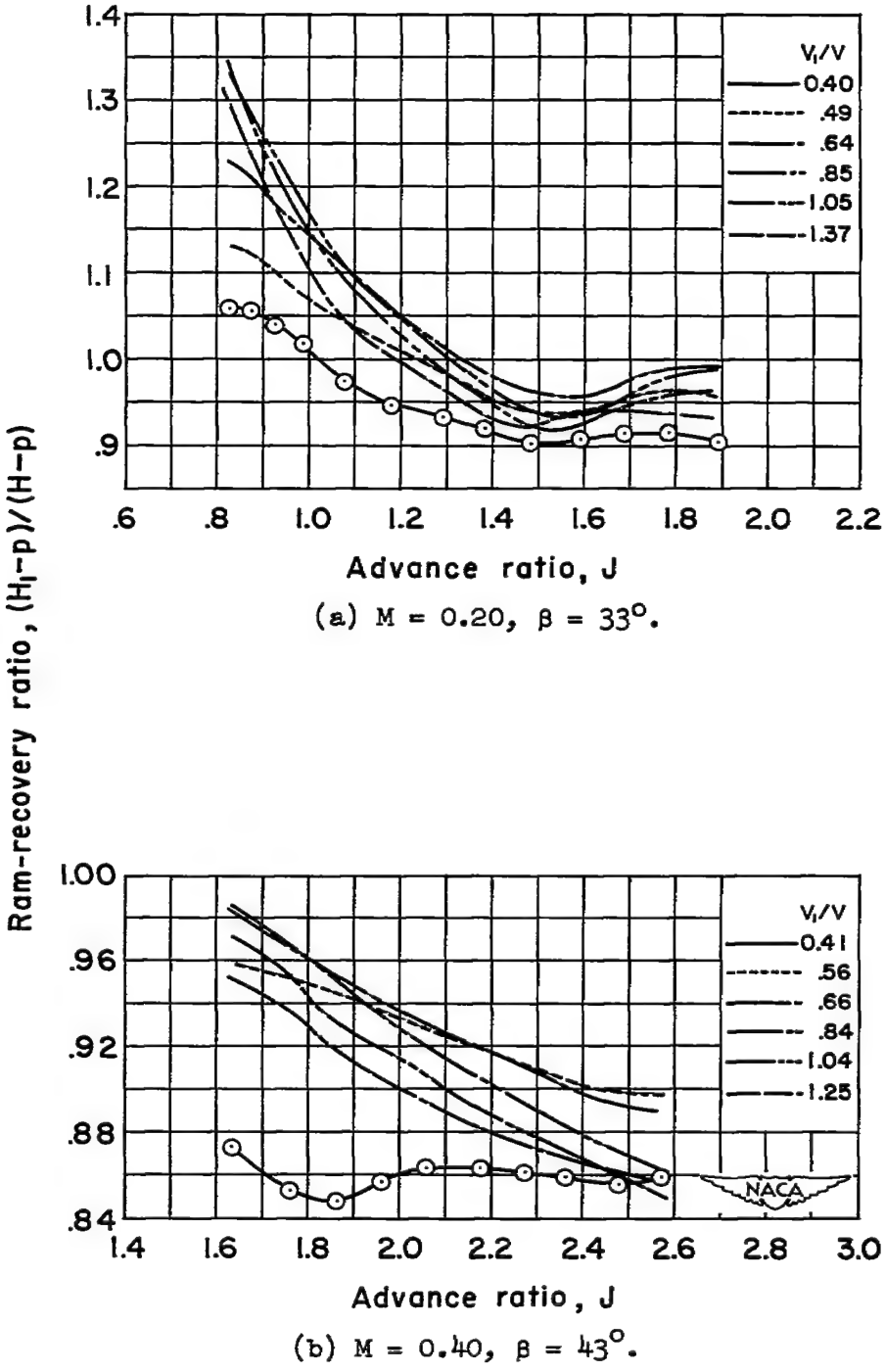

(a) M = 0.20, $\beta = 33^\circ$.

(b) M = 0.40, $\beta = 43^\circ$.

Figure 13.- The variation of the average ram-recovery ratio with advance ratio for various inlet velocity ratios, modified conical spinner.

[redacted]

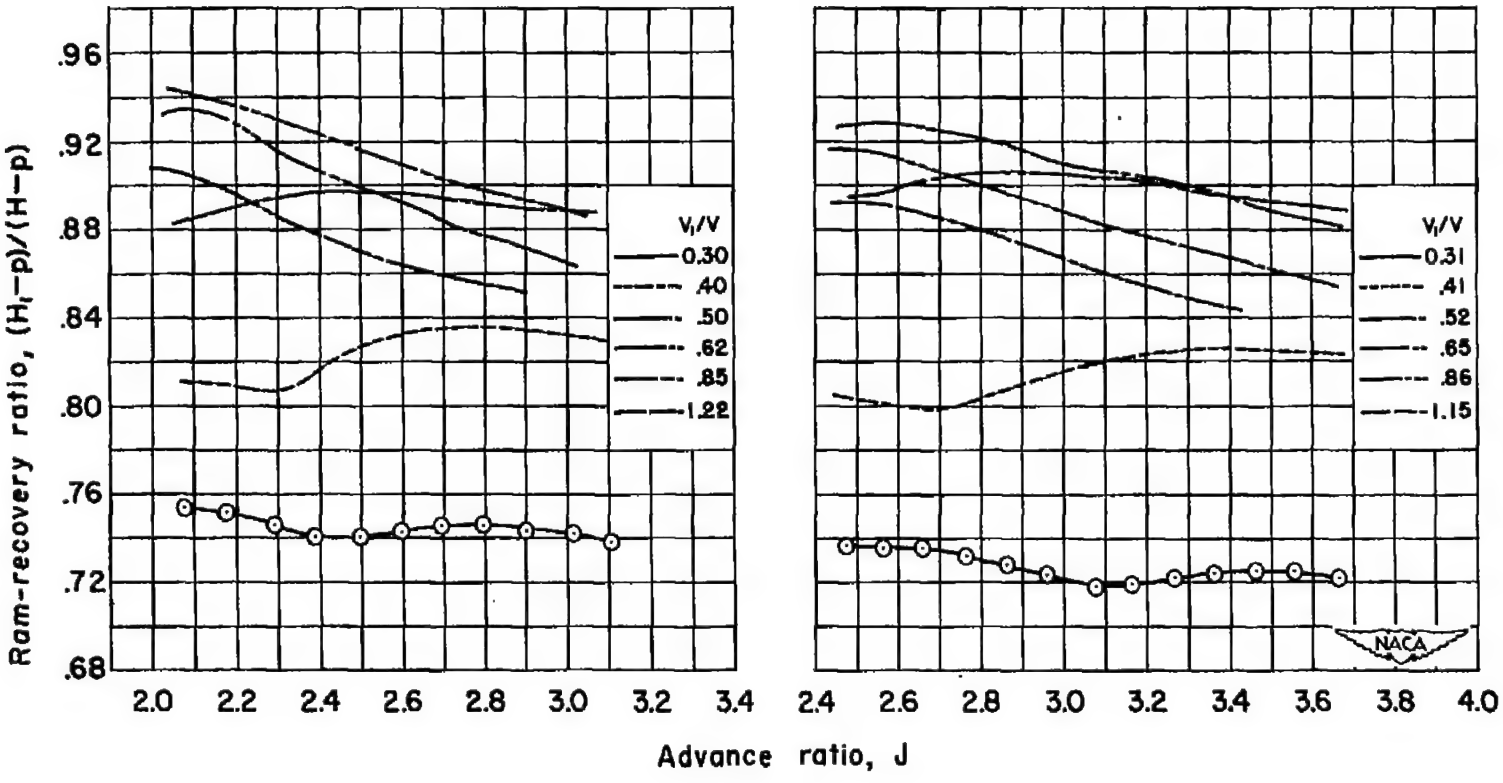

(c) M = 0.50, β = 48°.

(d) M = 0.60, β = 53°.

Figure 13.- Continued.

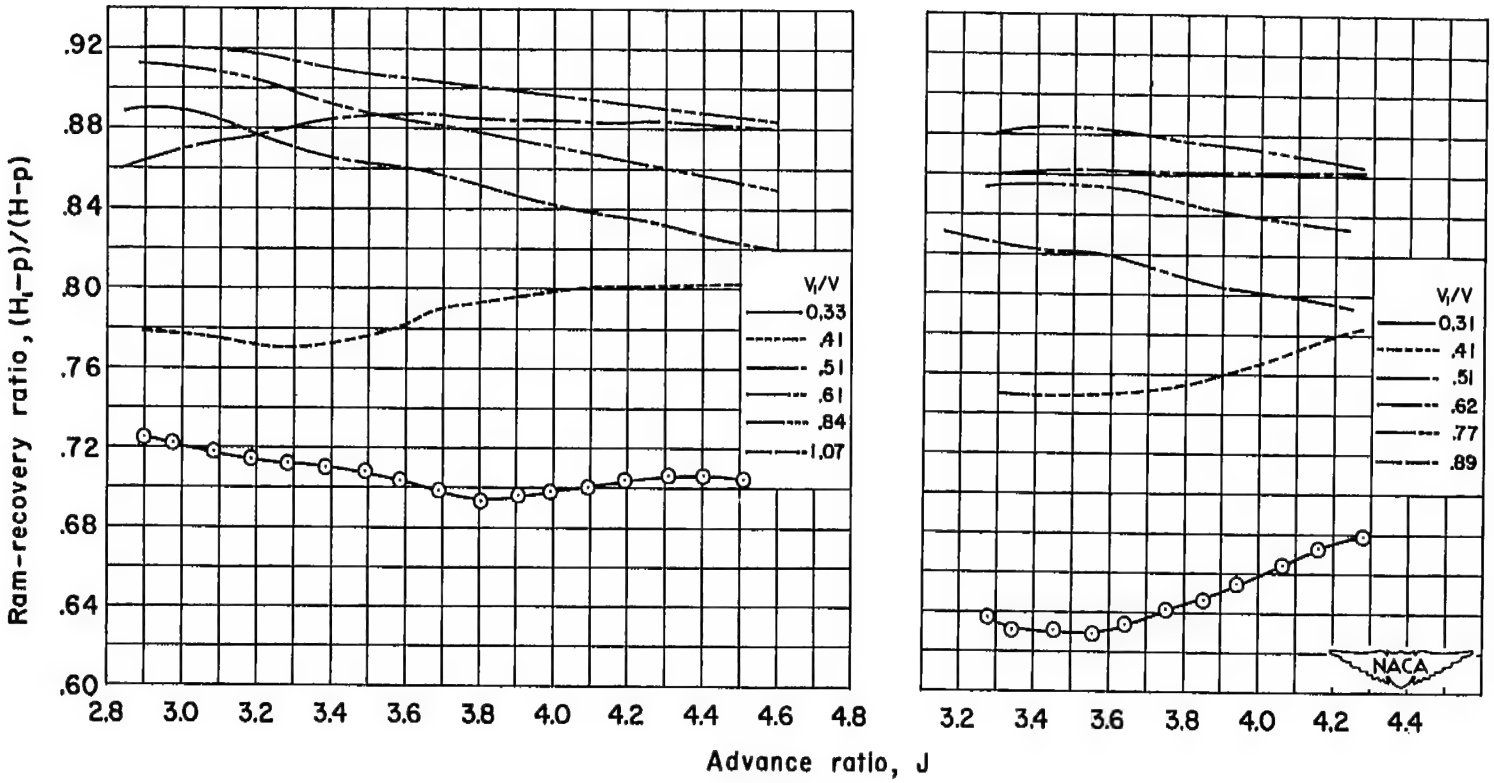

(e) M = 0.70, β = 58.5°.

(f) M = 0.80, β = 58.5°.

Figure 13.- Concluded.

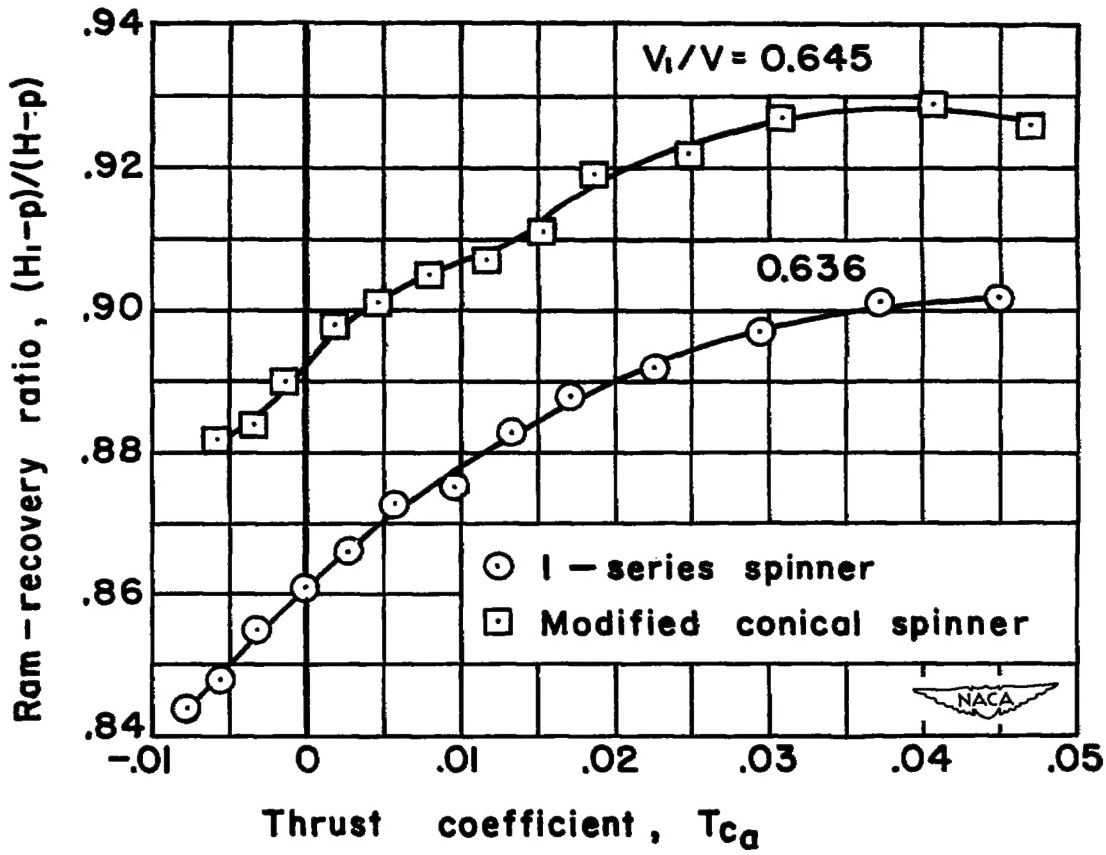

Figure 14.- Typical variation of ram-recovery ratio with propeller thrust coefficient; M = 0.60, $\beta = 53^{\circ}$.

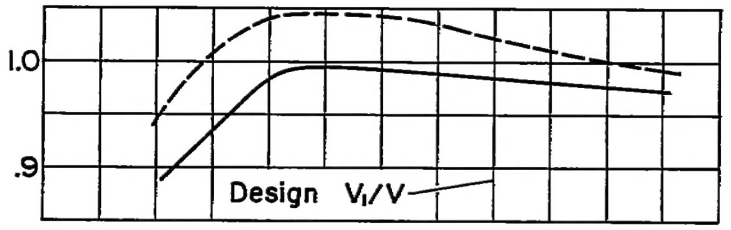

(a) M = 0.20, β = 33°, J = 1.22, T_{c_a} = 0.114.

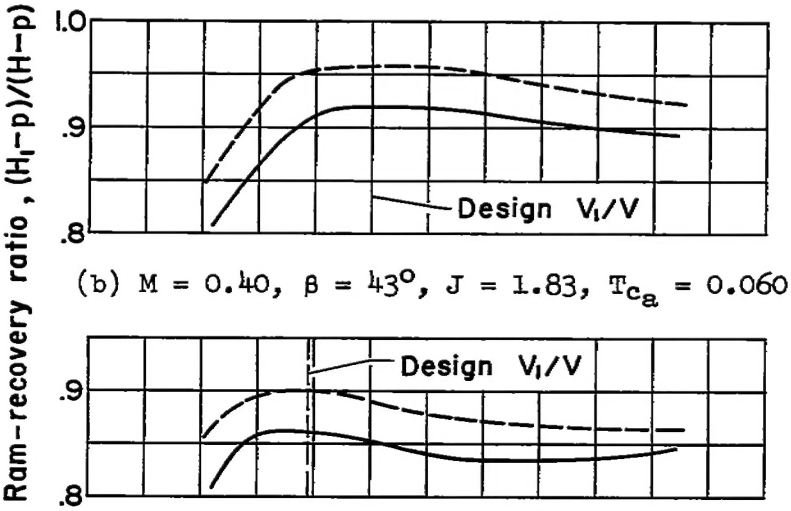

(b) M = 0.40, β = 43°, J = 1.83, T_{c_a} = 0.060.

(c) M = 0.40, β = 43°, J = 2.43, T_{c_a} = 0.000.

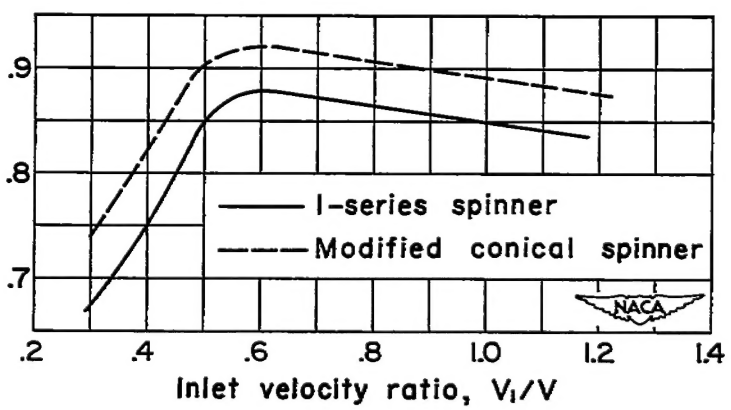

(d) M = 0.50, β = 48°, J = 2.45, T_{c_a} = 0.021.

Figure 15.- The effect of inlet velocity ratio on the average ram-recovery ratio for the cowl with 1-series and modified conical spinners, propeller operating.

[redacted]

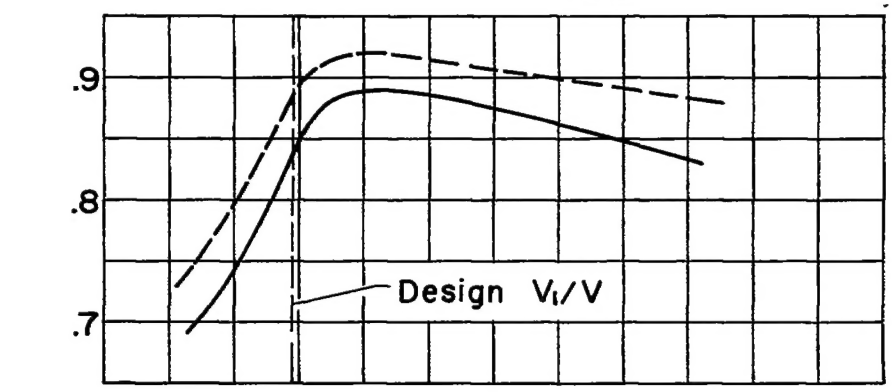

(e) M = 0.60, β = 53°, J = 2.82, T_{c_a} = 0.020.

(f) M = 0.70, β = 58.5°, J = 3.40, T_{c_a} = 0.016.

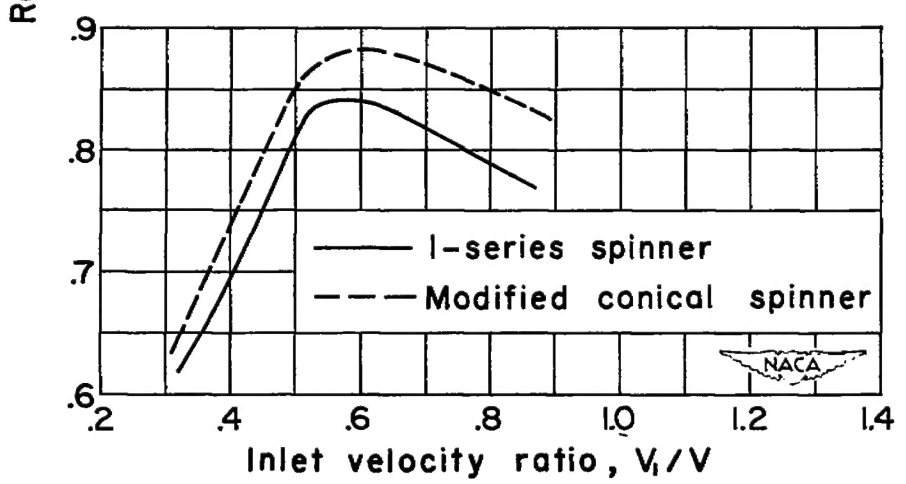

(g) M = 0.80, β = 58.5°, J = 3.30, T_{c_a} = 0.012.

Figure 15.- Concluded.

[redacted]